Theoretical Study on the Silylidyne Insertion into NH_3, H_2O, HF, PH_3, H_2S, and HCl

Z.-X. Wang and M.-B. Huang*

Graduate School at Beijing, University of Science and Technology of China, Academia Sinica, P.O. Box 3908, Beijing 100039, P. R. China

Received: July 2, 1997; In Final Form: October 15, 1997[⊗]

The reaction paths of the silylidyne insertion into NH_3, H_2O, HF, PH_3, H_2O, HF, and HCl have been studied by means of ab initio molecular orbital calculations incorporating electron correlation with Moller−Plesset perturbation theory up to the second and fourth order and using polarization basis sets augmented by diffuse functions. All these reactions involve the initial formation of an intermediate complex followed by a hydrogen-migration process via a transition state. Analyses for the reactivity of the six substrates in the SiH insertion reactions indicate that the reaction with the hydride of the right-hand group has a less stable complex and is more exothermic than with the hydride of the left-hand group and that the reaction with the second-row hydride has a lower overall barrier and is less exothermic than with the first-row hydride. Comparison with the CH and SiH_2 insertion reactions has been made, and it is noted that the CH, SiH_2, and SiH insertion reactions have similar reaction processes. The energetic results (for the barriers and reaction enthalpies) indicate that the SiH radical is less reactive than the CH radical in the insertion reactions.

Introduction

Recently silicon chemistry has attracted much attention due to its application to the production of thin silicon films and the etching of silicon wafers in microelectronics. The fundamental significance of silicon chemistry in manufacturing semiconductor material has stimulated extensive investigation. In 1995, an entire issue (Vol. 95, No. 5) of *Chemical Reviews* was devoted to the progresses in silicon chemistry. The present paper reports a theoretical study on the chemistry of the smallest silicon compound, silylidyne (SiH), which is known to be important in plasma chemical vapor deposition (CVD) processes.

In the literature, theoretical studies on the SiH reactions are very few though there are experimental (kinetic) studies.[1−4] The study of Gordon et al.[5] on the SiH + H_2 reaction is probably the only reported theoretical work on the SiH reactions. On the other hand we note in the literature that many SiH_2 reactions have been theoretically studied.[6] When we started theoretical studies[7,8] on the CH reactions, we also noted that theoretical studies on the CH reactions were much less than the studies[6b−6d,9] on the $^1CH_2$ reactions. This does not mean at all that the SiH and CH reactions are less important than the SiH_2 and CH_2 reactions.

In the present work we have investigated the SiH insertion reactions with NH_3, H_2O, HF, PH_3, H_2S, and HCl, which is part of our systematic theoretical study on the CH and SiH insertion reactions with the first- and second-row hydrides (groups IVA to VIIA). The SiH (and CH) insertion reactions into CH_4 and SiH_4 are presumably considered to be special[8] and will be investigated separately. Accurate ab initio calculations[10,5] for the CH and SiH insertions into H_2 have indicated that there is no energy barrier for the CH insertion but a substantial barrier for the SiH insertion, which is in agreement with experiment.[2] These facts imply that CH is more reactive than SiH in the insertion reaction into H_2. We will examine the reactivity of SiH and CH in the insertion reactions into hydrides based on the present study and our previous study[7] on the CH insertion reactions.

The SiH insertion reactions with NH_3, H_2O, HF, PH_3, H_2S, and HCl were investigated by using ab initio calculations. The mechanisms for these six SiH insertion reactions can be illustrated by the following eqs (1−6):

$$SiH + XH_n \rightarrow HSi{-}XH_n \rightarrow TS \rightarrow H_2SiXH_{n-1}$$

$$(1)\ X = N,\ n = 3; \quad (2)\ X = P,\ n = 3$$

$$(3)\ X = O,\ n = 2; \quad (4)\ X = S,\ n = 2$$

$$(5)\ X = F,\ n = 1; \quad (6)\ X = Cl,\ n = 1$$

As the CH and SiH_2 insertion reactions studied in refs 7 and 6a, these SiH insertion reactions involve the initial formation of an intermediate complex ($HSi{-}XH_n$), followed by a hydrogen-migration process via a transition state (TS) leading to the product H_2SiXH_{n-1}. In the present study we intend to give comparative discussion not only on the reactivity of the substrates (hydrides) in the SiH insertion reactions based on the present calculation results but also on the reactivity of the inserting species, SiH, CH, and SiH_2, based on the present and (ours and others) previous calculation results. We will simply mention the results in the previous studies[6a,7] on the CH and SiH_2 insertion reactions in the next two paragraphs.

In our previous study,[7] the insertion reactions of CH with NH_3, H_2O, and HF were investigated at the MP2(FULL)/6-31G(d,p) level. For each of these CH reactions the donor−acceptor intermediate complex, transition state, and insertion product all have negative relative energies to the respective reactants, which indicates that these CH reactions are feasible. In the present study we will compare the three CH insertion reactions with the respective SiH reactions.

Based on our and others' previous theoretical studies,[6c,8,9,11,12] it is known that the reaction processes of the CH and $^1CH_2$

* To whom correspondence may be addressed.

[⊗] Abstract published in *Advance ACS Abstracts,* December 1, 1997.

S1089-5639(97)02145-2 CCC: $15.00
Published on Web 01/01/1998

insertion are similar. It is natural to assume that the SiH and SiH_2 insertion reactions have similar reaction processes (see the above equations). The reaction paths of the SiH_2 insertion reactions with NH_3, PH_3, H_2O, H_2S, HF, and HCl were theoretically investigated at the HF/6-31G(d) level by Raghavachari et al.[6a] At their HF/6-31G(d) geometries of the reactants, intermediate complexes, transition states, and products, the single-point calculations were performed at the MP4SDQ/6-31G(d,p) level, and the effect of triple substitutions on correlation energy was estimated in their MP4SDTQ/6-31G(d) calculations (denoted as MP4SD(T)Q/6-31G(d,p) in the present paper). All the six SiH_2 insertion reactions were predicted to have substantial overall barriers.

Computational Methods

Standard ab initio molecular orbital calculations were performed using the Gaussian 94W suite of programs.[13] The structures of the reactants, complexes, transition states, and products were first optimized at the (U)HF/6-31G(d) level and then reoptimized in the (U)MP2(FC) calculations (second-order unrestricted Moller−Plesset perturbation theory[14] calculations with the core orbitals frozen) using the 6-31G(d,p), 6-31++G-(d,p), and 6-311++G(d,p) basis sets.[15] Frequency calculations were carried out at the (U)HF/6-31G(d) level in order to characterize stationary points in the potential energy surfaces as intermediate complexes or transition states and to evaluate zero-point energies (to be scaled by a factor of 0.9) for correcting the relative energies calculated at the various levels. To improve accuracy of the energetic results, the single-point calculations were performed at the MP4(FC)/6-311++G(2d,p)//MP2(FC)/6-311++G(d,p) level.

Additional calculations were carried out for the six reactions at the MP4(FC)SD(T)Q/6-31G(d,p)//HF/6-31G(d) level (see above and ref 6a).

For the open shell systems the expectation values of the S^2 operator have been examined. The values are 0.75−0.77 for the intermediate complexes and products and 0.80−0.87 for the transition states. The spin contaminations for the transition states are slightly large, and we note that there was a similar situation in the theoretical study[5] on the SiH + H_2 insertion reaction. The energetic results for the open shell systems at the post-SCF levels have been "spin-projected".

Results and Discussion

The potential energy curves shown in (parts A−F) of Figure 1 represent the calculated insertion reaction paths for reactions 1−6, respectively. The stationary points along the curves denoted as ***m*a**, ***m*b**, ***m*c**, and ***m*d** (***m*** = 1, 2, 3, 4, 5, and 6) represent the reactants, intermediate complexes, transition states, and insertion products of reactions 1−6, respectively, and the MP4(FC)/6-311++G(2d,p)//MP2(FC)/6-311++G(d,p) relative energies (corrected with the scaled HF/6-31G(d) zero-point energies) of ***m*b**, ***m*c**, and ***m*d** to ***m*a** (respectively) are given in Figure 1. The structures of ***m*b**, ***m*c**, and ***m*d**, optimized at the HF/6-31G(d), MP2(FC)/6-31G(d,p), MP2(FC)/6-31++G(d,p), and MP2(FC)/6-311++G(d,p) levels, are given in Figure 2. In Table 1 listed are the relative energies calculated at the various levels, together with the ((U)MP2 (FC)/6-311++G(d,p)) $\langle S^2 \rangle$ values, the (HF/6-31G(d)) zero-point energies, and the (HF/6-31G(d)) imaginary frequencies for the transition states. The relative energies given in Table 1 have included the scaled zero-point energy corrections. The relative energies of ***m*b**, ***m*c**, and ***m*d** (***m*** = 1−6, 18 species in total) imply that the calculations at the various (SCF and four post-SCF) levels all predict the same skeleton (shown in Figure 1) of the energy profiles for each of the SiH insertion reactions. As shown in Figure 2, the optimization calculations at the SCF and three post-SCF levels predict similar geometries for each of the 18 species. It is noted in Table 1 that the post-SCF calculations (at the four levels) predict much lower barriers than the SCF calculations and that the post-SCF calculations with diffuse functions included in the basis sets (at the three levels) predict close values of the relative energy for each of the 18 species. The term " relative energy" (of a species) in the present article means "relative energy of a species to the reactants in the same reaction". In the following two subsections the MP4(FC)/6-311++G(2d,p)//MP2(FC)/6-311++G(d,p) energetic results (in Table 1 and Figure 1) and the MP2(FC)/6-311++G(d,p) geometrical results (in Figure 2) are used.

We will first describe and discuss the results for the SiH insertion reactions in subsections 1 and 2, and then compare the reaction paths of the SiH insertion with those of the CH and SiH_2 insertion in subsections 3 and 4.

1. Results for the SiH Insertion Reactions. As mentioned above, the general calculation results for reactions 1−6 are given in Table 1 and Figures 1 and 2. There are no available experimental data for these reactions.

Insertion into NH_3 and PH_3. For reactions 1 and 2, the binding energies of the initially formed complexes are 20.3 and 18.9 kcal/mol and the reaction enthalpies are 45.3 and 39.1 kcal/mol, respectively. The overall barrier for reaction 1 is 7.1 kcal/mol, while the transition state for reaction 2 has a negative relative energy value of −2.4 kcal/mol.

It is known[7] that the interaction between the empty p-orbital on the inserting species and the lone-pair orbital on the substrate causes the lone-pair donation that stabilizes the intermediate complex (donor−acceptor complex) initially formed in the insertion reaction. In the structures of **1b** and **2b** (see Figure 2), the near-orthogonal HSiX (X = N and P) angles and the orientations of the XH bonds imply that a silicon p-orbital is directed at the lone pairs orbitals on the X-atoms. The similar geometrical features of the structures of **3b**, **4b**, **5b**, and **6b** (see Figure 2) also imply the interaction between the silicon p-orbital and the lone pair orbitals on the X-atoms (X = O, S, F, and Cl).

The Si−N distances in **1b**, **1c**, and **1d** are 2.097, 1.891, and 1.727 Å, respectively, and the values are reasonably in a decreasing order. The Si−P distances in **2b**, **2c**, and **2d** are 2.346, 2.853, and 2.256 Å, respectively, and the values are not in a decreasing order. It is noted in ref 6a that the Si−P distance in the transition state for the SiH_2 insertion into PH_3 was also predicted to be longer than the distances in the complex and in the product.

The HF/6-31G(d) frequency calculations predict a (unique) imaginary frequency value of 1993.0i cm^{-1} for **1c** and a value of 1047.1i cm^{-1} for **2c.** In the structure of **1c** the attacked N−H bond is elongated by 38% relative to the length in NH_3, while in the structure of **2c** the attacked P−H bond is elongated by only about 3% relative to the length in PH_3.

The complex **1b** is 20.3 and 27.4 kcal/mol lower in energy than **1a** and **1c**, respectively, which indicates that it lies in a deep minimum in the potential energy surface and might have a significant lifetime to be an observable species spectroscopically.

Insertion into H_2O and H_2S. For reactions 3 and 4, the binding energies of the complexes are 9.8 and 10.7 kcal/mol and the reaction enthalpies are 52.3 and 45.7 kcal/mol, respectively. The transition state **3c** has a positive relative

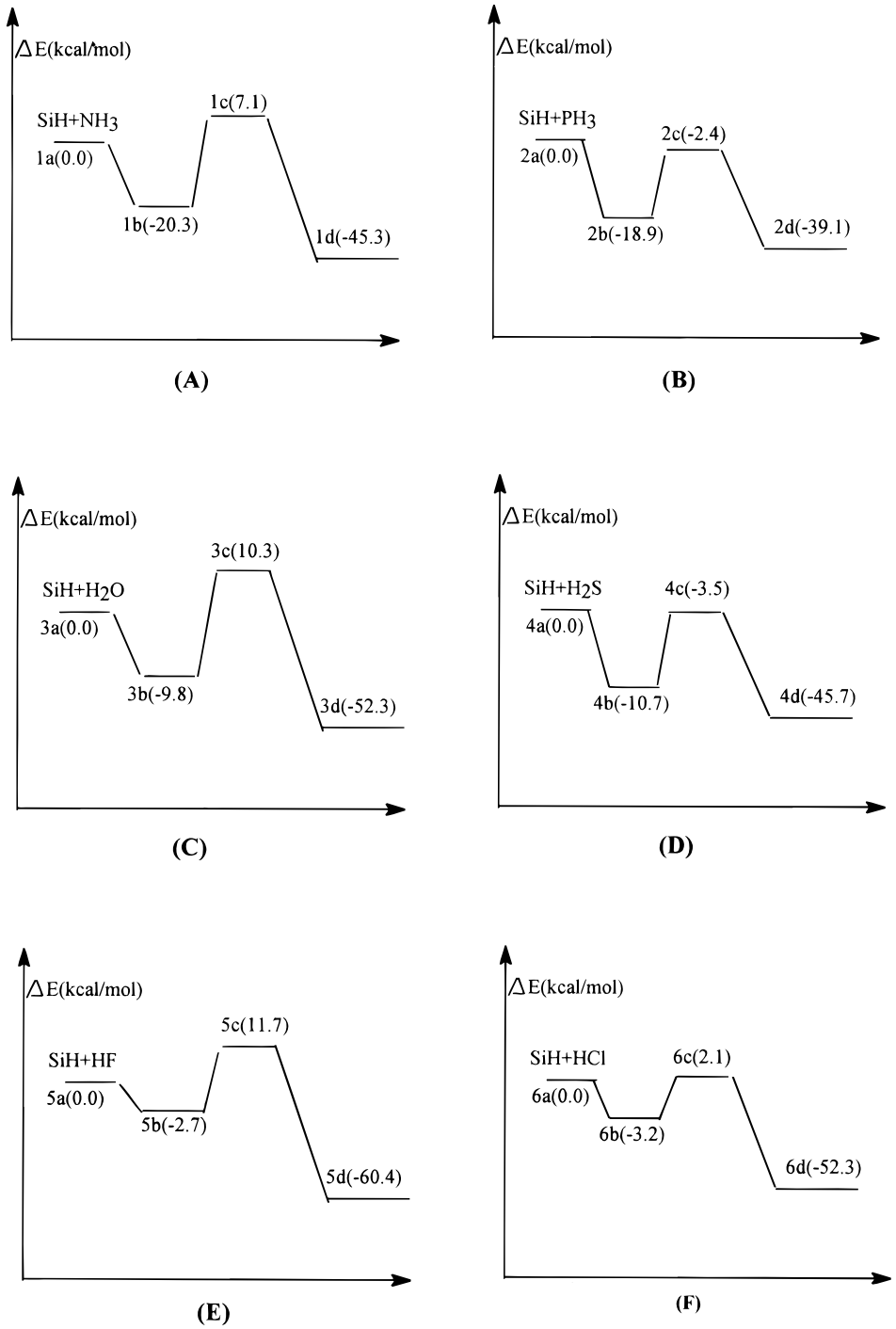

Figure 1. Schematic diagram of the potential energy curves of the SiH insertion reactions with NH_3 (A), H_2O (C), HF (E), PH_3 (B), H_2S (D), and HCl (F). The values in parentheses are the MP4(FC)/6-311++G(2d,p)//MP2(FC)/6-311++G(d,p) relative energies in kcal/mol (corrected with the scaled HF/6-31G(d) zero-point energies).

energy value of 10.3 kcal/mol, while the transition state **4c** has a negative relative energy value of −3.5 kcal/mol. The Si−O distances in **3b**, **3c**, and **3d** are 2.180, 1.889, and 1.670 Å, respectively. The Si−S distances in **4b**, **4c**, and **4d** are 2.519, 2.393, and 2.138 Å, respectively.

The HF/6-31G(d) frequency calculations for the transition states **3c** and **4c** predict the (unique) imaginary frequency values of 1855.0i and 1500.0i cm^{-1}, respectively. In the structures of **3c** and **4c** the attacked X−H (X = O and S) bonds are elongated by 38% and 17% relative to the X−H lengths in the H_2X molecules, respectively.

Insertion into HF and HCl. The relative energies of **5b**, **5c**, and **5d** in reaction 5 are −2.7, 11.1, and −60.4 kcal/mol, and the Si−F distances in their structures are 2.545, 1.934, and 1.628 Å, respectively. The relative energies of **6b**, **6c**, and **6d** in reaction 6 are −3.2, 2.2, and −52.3 kcal/mol, and the Si−Cl distances in their structures are 2.890, 2.433, and 2.058 Å, respectively. It is noted that **6c** has a small positive relative energy value (**2c** and **4c** have negative relative energy values) and that the Si−F distance in **5b** is very long.

The HF/6-31G(d) frequency calculations for **5c** and **6c** predict the (unique) imaginary frequency values of 1820.0i and 1162.6i cm^{-1}, respectively. In the structures of **5c** and **6c** the attacked X−H (X = F and Cl) bonds are elongated by 33% and 19% relative to the X−H lengths in the HX molecules, respectively.

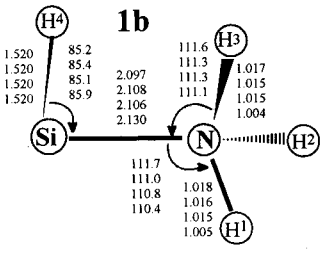

∠H²NSiH¹=	∠H³NSiH¹=	∠H⁴SiNH¹=
120.2	-120.2	180.0
120.1	-120.1	180.0
120.0	-120.0	179.8
119.8	-119.8	180.0

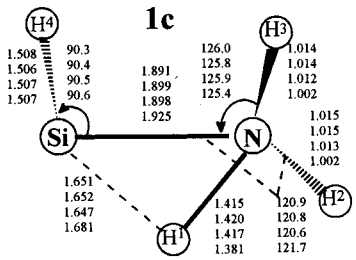

∠H²NSiH¹=	∠H³NSiH¹=	∠H⁴SiNH¹=
88.3	-102.0	94.1
88.6	-102.2	94.4
88.0	-101.8	94.1
87.1	-94.3	93.7

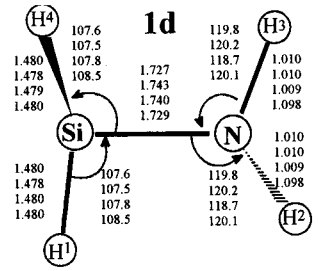

∠H²NSiH¹=	∠H³NSiH¹=	∠H⁴SiNH¹=
49.2	-169.2	119.9
47.8	-167.8	119.9
50.9	-170.2	119.1
47.6	-168.1	119.8

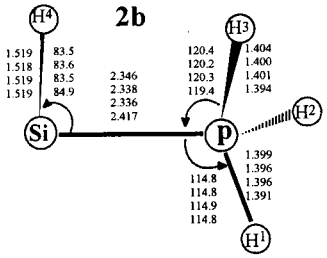

∠H²PSiH¹=	∠H³PSiH¹=	∠H⁴SiPH¹=
118.4	-118.4	180.0
118.5	-118.5	179.8
118.6	-118.5	180.1
118.6	-118.6	179.9

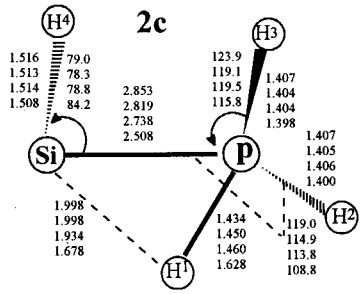

∠H²PSiH¹=	∠H³PSiH¹=	∠H⁴SiPH¹=
64.5	-58.0	89.1
59.9	-64.0	96.5
60.9	-52.4	96.3
61.3	-47.5	93.5

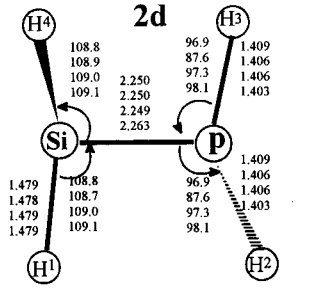

∠H²PSiH¹=	∠H³PSiH¹=	∠H⁴SiPH¹=
72.2	168.8	119.1
72.0	169.0	119.0
72.2	168.7	119.0
71.7	168.9	119.2

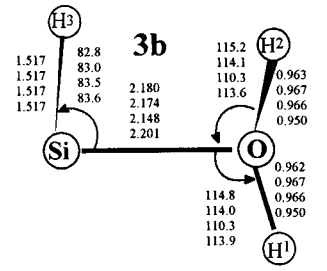

∠H²OSiH¹=	∠H³SiOH¹=
-123.7	155.0
-124.0	157.3
-117.5	152.9
-123.9	155.5

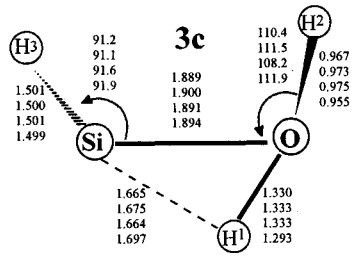

∠H²OSiH¹=	∠H³SiOH¹=
-88.1	-97.6
-90.7	-97.7
-89.1	-97.0
-91.0	-95.6

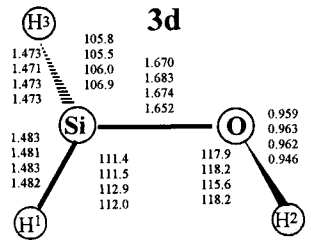

∠H²OSiH¹=	∠H³SiOH¹=
-55.0	-120.6
-55.6	-120.6
-63.9	-120.2
-62.5	-120.4

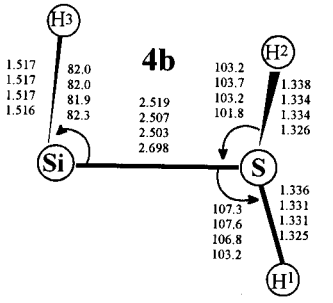

∠H²SSiH¹=	∠H³SiSH¹=
-97.2	166.3
-98.2	168.3
-97.7	170.7
-97.9	168.6

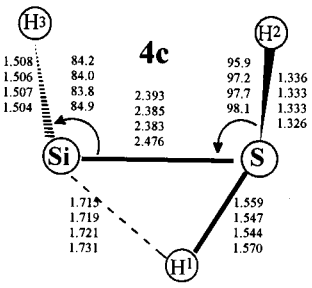

∠H²SSiH¹=	∠H³SiSH¹=
-80.5	-92.1
-81.0	-92.3
-80.8	-92.6
-81.4	-94.7

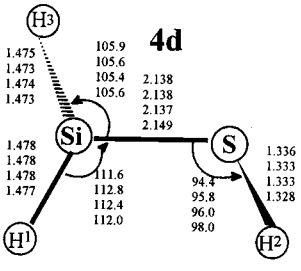

∠H²SSiH¹=	∠H³SiSH¹=
-55.1	-120.6
-55.7	-120.6
-56.9	-120.5
-59.1	-120.5

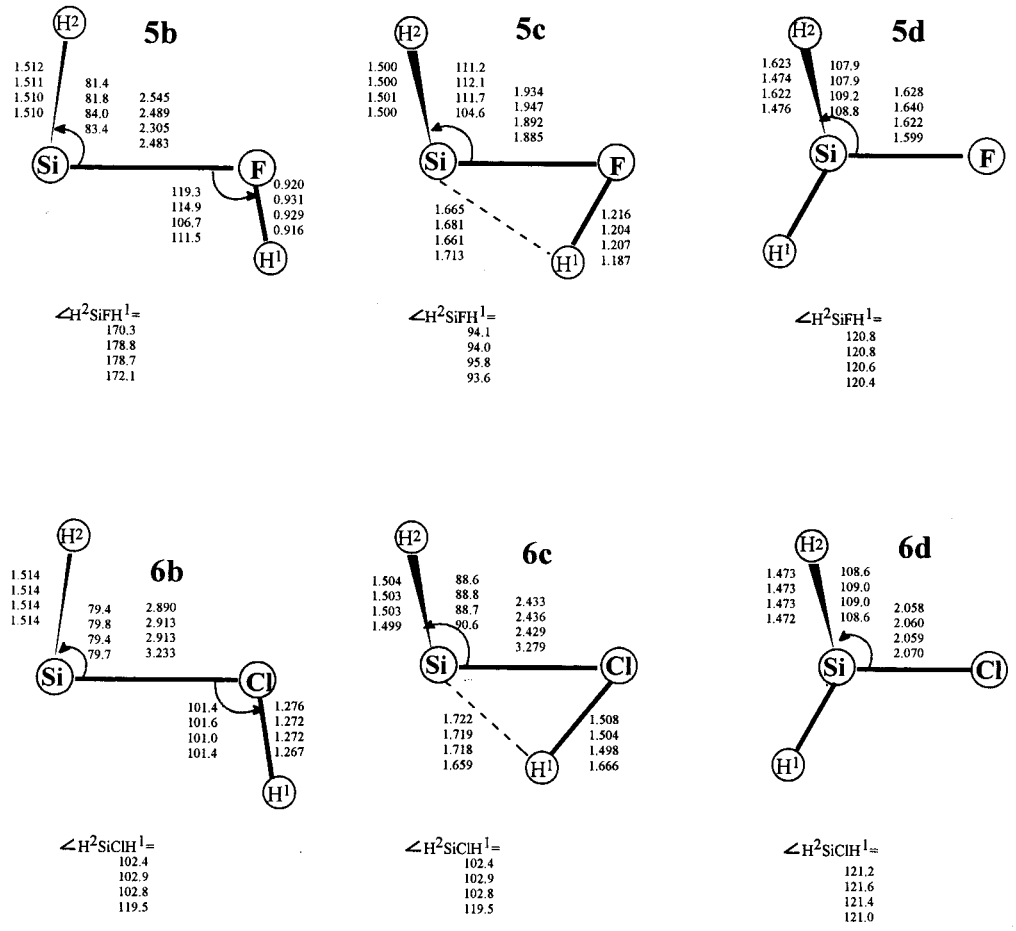

Figure 2. Optimized structures of the intermediate complexes (***m*b**), transition states (***m*c**), and products (***m*d**) for the SiH insertion reactions with NH_3 (eq 1), H_2O (eq 3), HF (eq 5), PH_3 (eq 2), H_2S (eq 4), and HCl (eq 6). The values given in the first, second, third, and fourth rows are the parameters optimized at the MP2(FC)/6-311++G(d,p), MP2(FC)/6-31++G(d,p), MP2(FC)/6-31G(d,p), and HF/6-31G(d) levels, respectively. Bond lengths are given in Å and angles in deg.

2. Discussion on Reactivity of the Substrates. On the basis of the results for the SiH insertion reactions into the first-row hydrides (reactions 1, 3, and 5), we could make the following remarks. As the X-atom (the central atom of hydride) moves from left to right (from N to F) across the first row in the periodic table, (i) the binding energy of the intermediate complex $HSiXH_n$ initially formed in the insertion reaction decreases and the Si-X distance in the structure of the complex increases (though the radius of the X-atom decreases); (ii) the overall barrier (the relative energy of the transition state) increases; and (iii) the reaction enthalpy of the insertion reaction (the relative energy of the insertion product) increases and the Si−X bond distance in the structure of the product decreases. Point i (the complex becomes less stable as the atomic number of the X-atom increases) could be explained by the fact that the higher the electronegativity of the X-atom, the more difficult it is to donate its lone-pair electron to the empty silicon p-orbital. As stated in points i and iii, the Si−X distance increases in the complexes and decreases in the products with the atomic number of the X-atom. This is apparently because the type of interaction between the SiH and XH_n fragments in the complexes is different from that in the products.

On the basis of the results for the SiH insertion reactions into the second-row hydrides (reactions 2, 4, and 6), we could make the same remarks as for the insertions into the first-row hydrides except point ii. The relative energies of **2c**, **4c**, and **6c** (see Table 1) are not in an increasing order, and the value (−2.4 kcal/mol) for **2c** is slightly higher than the value (−3.5 kcal/mol) for **4c**.

The X-atoms in the six reaction substrates belong to group VA, VIA, or VIIA in the periodic table. We now examine changes in the features of the insertion reaction path when the X-atom drops from the first row to the second in the same group. When the X-atom drops in each of the three groups, (i) the binding energy of the intermediate complex does not change significantly; (ii) the overall barrier for the insertion reaction decreases, and the attacked X−H bond in the structure of the transition state is elongated to less extent (the percentages of elongation decrease from around 40% to around 15%); and (iii) the reaction enthalpy of the insertion reaction decreases. Point i means that the complexes containing the second-row X-atoms are not significantly more stable than those containing the first-row X atoms and implies that the previously proposed rule (the lower the electronegativity of the X-atom, the more stable the complex containing it) does not hold across a group in which the X-atoms in different rows have significantly different radii. Point ii implies a correlation between the barrier height and the length of the attacked X−H bonds: the higher barrier is correlated with the larger percentage of elongation of the attacked X−H bond in the transition state structure, and we have noted similar correlation rules suggested in refs 6a and 6b.

3. Comparison between the SiH and CH Insertion Reactions. The insertion reactions of CH into NH_3, H_2O, and

TABLE 1: Relative Energies[a] (in kcal/mol) for the Intermediate Complexes, Transition States, and Products of the SiH Insertion Reactions with NH_3, PH_3, H_2O, H_2S, HF, and HCl, Together with the HF/6-31G(d) Zero-Point Energies (ZPE, in kcal/mol), the (U)MP2/6-311++G(d,p) $\langle S^2 \rangle$ Value, and the Imaginary Frequencies (IMG, in cm^{-1}) for the Transition States

		ZPE	$\langle S^2 \rangle$	IMG	HF/6-31G(d)	MP2/6-31G(d,p)[b]	MP2/6-31++G(d,p)	MP2/6-311++G(d,p)	MP4/6-311++G(2d,p)[c]
SiH + NH_3	**1a**	26.3			0.0	0.0	0.0	0.0	0.0
					(−345.59422)[d]	(−345.85543)	(−345.86628)	(−345.91233)	(−345.97491)
HSi−NH_3	**1b**	30.3	0.76		−19.2	−25.2	−22.7	−22.2	−20.3
TS	**1c**	25.6	0.82	1993.0i	22.5	6.7	7.2	5.9	7.1
H_2SiNH_2	**1d**	27.3	0.76		−42.5	−47.4	−47.6	−48.7	−45.3
SiH + PH_3	**2a**	19.5			0.0	0.0	0.0	0.0	0.0
					(−631.85782)	(−632.05079)	(−632.05427)	(−632.11003)	(−632.18548)
HSi−PH_3	**2b**	22.8	0.77		−11.0	−19.6	−19.7	−18.9	−18.9
TS	**2c**	20.3	0.78	1047.1i	13.9	−0.9	−1.2	−2.1	−2.4
H_2SiPH_2	**2d**	22.3	0.76		−36.0	−42.6	−42.6	−41.9	−39.1
SiH + H_2O	**3a**	17.4			0.0	0.0	0.0	0.0	0.0
					(−365.42061)	(−365.69198)	(−365.70712)	(−365.77173)	(−365.83095)
HSi−OH_2	**3b**	20.6	0.77		−9.7	−14.8	−11.9	−11.2	−9.8
TS	**3c**	17.1	0.85	1855.0i	25.6	8.6	10.7	11.9	10.3
H_2SiOH	**3d**	19.5	0.75		−52.3	−55.4	−53.8	−52.5	−52.3
SiH + H_2S	**4a**	13.4			0.0	0.0	0.0	0.0	0.0
					(−688.07118)	(−688.28231)	(−688.28596)	(−688.34453)	(−688.41992)
HSi−SH_2	**4b**	16.1	0.77		−4.5	−9.9	−10.2	−10.1	−10.7
TS	**4c**	14.3	0.80	1500.0i	16.2	−1.1	−1.4	−3.0	−3.5
H_2SiSH	**4d**	16.7	0.76		−44.0	−49.1	−46.8	−48.2	−45.7
SiH + HF	**5a**	9.3			0.0	0.0	0.0	0.0	0.0
					(−389.41277)	(−389.66685)	(−389.68966)	(−389.77570)	(−389.83562)
HSi−FH	**5b**	10.9	0.77	1820.0i	−4.0	−11.2	−3.6	−3.2	−2.7
TS	**5c**	8.4	0.86		22.2	18.8	9.4	13.2	11.1
H_2SiF	**5d**	12.0	0.75		−66.7	−67.3	−63.2	−58.8	−60.4
SiH + HCl	**6a**	7.7			0.0	0.0	0.0	0.0	0
					(−749.46984)	(−749.67746)	(−749.68510)	(−749.74173)	(−749.81478)
HSi−ClH	**6b**	8.8	0.77		−0.8	−2.0	−3.0	−3.0	−3.2
TS	**6c**	6.2	0.84	1162.6i	16.0	4.7	4.5	2.3	2.2
H_2SiCl	**6d**	11.3	0.75		−55.0	−56.0	−55.7	−54.7	−52.3

[a] All the relative energies have included the scaled (by a factor of 0.9) HF/6-31G(d) ZPE corrections. [b] The MPn calculations were carried out with the core orbital frozen, and the spin-projected energetic results are used. [c] Single-point calculations at the MP2/6-311++G(d,p) geometries. [d] Values in parentheses are the total energies in au.

HF were investigated at the MP2(FULL)/6-31G(d,p) level.[7] The CH + NH_3 and CH + H_2O insertion reactions were also investigated at the MP2(FC)/6-31G(d,p) level in our recent study,[16] and the MP2(FULL) and MP2(FC) calculations predict almost identical results for the reaction paths. The following comparative discussion on the SiH and CH insertion reactions with NH_3, H_2O, and HF is based on the MP2(FULL)/6-31G(d,p) results [7] for the three CH insertion reactions and the MP2(FC)/6-31G(d,p) results for the three SiH insertion reactions reported in the present paper.

Since the SiH and CH radicals have the same valence electronic structure, it is not surprising to note that the skeletons of the energy profiles for the three SiH insertion reactions are similar to those for the three CH insertion reactions,[7] respectively. For the three CH insertion reactions the transition states all have negative relative energies,[7] while for the three SiH insertion reactions the transition states all have positive relative energies, which indicates that the CH insertion into these three molecules is more feasible than the SiH insertion. The insertion reactions of CH and SiH into H_2 have been studied by Brooks et al.[10] and by Gordon et al.,[5] respectively, and their accurate calculations indicate that there is a substantial energy barrier for the SiH insertion but no barrier for the CH insertion. Their results support the above conclusion on the insertion reactivity of CH and SiH. In the structures of the transition states for the CH insertion, the attacked X−H bonds (X = N, O, and F) are elongated by about 16% while the corresponding percentages in the cases of the SiH insertion are about 38% (at the MP2(FC)/6-31G(d,p) level). The binding energies of the intermediate complexes HC−XH_n (X = N, O, and F) are 26.5, 12.0, and 5.8 kcal/mol (at the (U)MP2(FULL)/6-31G(d,p) + ZPE level), respectively, while those of the complexes HSi-XH_n (X = N, O, and F) are 25.2, 14.8, and 11.2 kcal/mol (at the (P)MP2(FC)/6-31G(d,p) + ZPE level), respectively. The reaction enthalpies for the three CH insertion reactions are dozens of kcal/mol larger than the values for the three SiH insertion reactions, respectively. The energetic results (for the barriers and reaction enthalpies) indicate that the SiH radical is less reactive than the CH radical in the insertion reactions.

It has been reported in the theoretical studies for the $^1CH_2$ and SiH_2 insertion reactions that there are multiple bonds in the complexes formed between $^1CH_2$ and the second-row hydrides. In the present study we have found no multiple bonds in the complexes HSi−XH_n (X = N, O, F, P, S, and Cl). In our previous study[7] on the CH insertion reactions with NH_3, H_2O, and HF, we found no multiple bonds in the complexes HC−XH_n (X = N, O, and F). In our recent study[17] on the CH insertion reactions with PH_3, H_2S, and HCl, the complex HC−PH_3 was predicted to have a large binding energy and the predicted C−P bond length in this complex is significantly shorter than that in the insertion product H_2C-PH_2. (We also mention that the predicted C−X lengths in the complexes HC−XH_n (X = P, S, and Cl) are all shorter than those in the respective transition states and that the energetic results also support the above conclusion on the insertion reactivity of CH and SiH.)

4. Comparison between the SiH and SiH_2 Insertion Reactions. As mentioned in Introduction, the SiH_2 insertion reactions with NH_3, H_2O, HF, PH_3, H_2S, and HCl were studied by Raghavachari et al.[6a] in 1984. In their study, the reaction

TABLE 2: MP4SD(T)Q/6-31G(d,p)//HF/6-31G(d) Relative Energies (in kcal/mol), Including the HF/6-31G(d) Zero-Point Energy Corrections, for the Intermediate Complexes (IM) and Transition States (TS) in the SiH_2 and SiH Insertion Reactions with the XH_n Molecules

		NH_3	H_2O	HF	PH_3	H_2S	HCl
SiH_2[a]	IM	−25.1	−13.0	−7.0	−18.0	−9.0	−2.0
	TS	13.0	9.0	3.0	2.0	5.0	6.0
SiH[a,b]	IM	−22.6	−12.4	−3.4	−16.4	−6.6	−1.0
	TS	14.0	14.0	12.1	1.7	3.3	14.5

[a] See ref 6a. [b] For the SiH reactions the MP4(FC)SD(T)Q/6-31G(d,p)//HF/6-31G(d) calculations were carried out, and the spin-projected energetic results are used. The relative energies also include the HF/6-31G(d) zero-point energy ZPE corrections.

paths were calculated only at the HF/6−31(d) level and the single-point MP4SD(T)Q/6-31G(d,p)//HF/6-31G(d) (see above) calculations were carried out for the final energetic results. For comparison between the SiH_2 and SiH insertion reactions we performed additional single-point calculations for the six SiH insertion reactions.

As shown in the figures of ref 6a, the skeletons of the energy profiles for the SiH_2 insertion reactions with NH_3, H_2O, HF, PH_3, H_2S, and HCl are similar to those for the respective SiH insertion reactions. The MP4SD(T)Q/6-31G(d,p)//HF/6-31G-(d) relative energies for the intermediate complexes and transition states in the SiH_2 and SiH insertion reactions are given in Table 2. Since SiH_2, unlike CH, has one more hydrogen atom than SiH, it is meaningless to compare the relative energy values and geometries of the complexes and transition states for the SiH_2 insertion reactions with those for the SiH insertion reactions. The relative energies of the transition states for the SiH insertion reactions with PH_3 and H_2S, reported in Table 2, are small positive values, while the relative energies of these two transition states predicted at the MP2(FC)/6-31++G(d,p), MP2(FC)/6-311++G(d,p), and MP4(FC)/6-311++G(2d,p)//MP2(FC)/6-311++G(d,p) levels are small negative values (see Table 1). As shown in Table 2, the relative energies of the transition states for the SiH_2 insertion reactions with PH_3 and H_2S (also with HF and HCl) are also small positive values, and at more sophisticated levels of theory these transition states might be predicted to have negative relative energies.

Conclusion

The SiH insertion reactions with NH_3, H_2O, HF, PH_3, H_2S, and HCl have been studied at the HF/6-31G(d), MP2/6-31G-(d,p), MP2/6-31++G(d,p), MP2/6-311++G(d,p) and MP4/6-311++G(2d,p)//MP2/6-311++G(d,p) levels. All these insertion reactions involve the initial formation of an intermediate complex followed by a hydrogen-migration process via a transition state leading to the insertion product. Analyses for the reactivity of the six substrates (hydrides) in the SiH insertion reactions indicate that the reaction with the hydride of the right-hand group in the periodic table has a less stable complex and is more exothermic than with the hydride of the left-hand group and that the reaction with the second-row hydride has a lower overall barrier and is less exothermic than with the first-row hydride. Comparison with the CH and SiH_2 insertion reactions has been made, and it is noted that the CH, SiH_2, and SiH insertion reactions have similar reaction processes. The energetic results (for the barriers and reaction enthalpies) indicate that the SiH radical is less reactive than the CH radical in the insertion reactions.

Acknowledgment. We appreciate the financial support of this work that was provided by the National Natural Science Foundation Committee of China.

References and Notes

(1) Schmitt, J. P. M.; Gressier, P.; Krishnan, M.; DeRosny, G.; Perrin, K.P. *J. Chem. Phys.* **1984**, *84*, 281.

(2) Begemann, M. H.; Dreyfus, R. W.; Jasinski, J. M. *Chem. Phys. Lett.* **1989**, *155* (4,5), 351.

(3) Nemoto, M.; Suzuki, A.; Nakamura, H.; Shibuya, K.; Obi, K. *Chem. Phys. Lett.* **1989**, *162* (6), 467.

(4) Nomura, H.; Akimoto, K.; Kono, A.; Goto, T. *J. Phys. D: Appl. Phys.* **1995**, *28*, 1977.

(5) Gordon, M. S.; Xie, Y.; Yamaguchi, Y.; Grev, R. S.; Schaefer, H. F. *J. Am. Chem. Soc.* **1993**, *115*, 1503.

(6) (a) Raghavachari, K.; Chandrasekhar, J.; Gordon, M. S.; Dykema, K. J. *J. Am. Chem. Soc.* **1984**, *106*, 5853 and references therein. (b) Gano; D. R.; Gordon, M. S.; Boatz, J. A. *J. Am. Chem. Soc.* **1991**, *113*, 6711. (c) Gordon, M. S.; Gano, D. R. *J. Am. Chem. Soc.* **1984**, *106*, 5421. (d) Sosa, C.; Schlegel, H. B. *J. Am. Chem. Soc.* **1984**, *106*, 5847. (e) Becerra, R.; Frey, H. M.; Mason, B. P.; Walsh, R.; Gordon, M. S. *J. Chem. Soc., Faraday Trans.* **1995**, *91* (17), 2723. (f) Roenigk, K. F.; Jensen, K. F.; Carr, R. W. *J. Phys. Chem.* **1987**, *91*, 5726 (g) Sakai, S.; Nakamura, M. *J. Phys. Chem.* **1993**, *97*, 4960.

(7) Wang, Z.-X.; Liu, R.-Z.; Huang, M.-B.; Yu, Z. *Can. J. Chem.* **1996**, *74*, 910.

(8) Wang, Z.-X.; Huang, M.-B.; Liu, R.-Z. *Can. J. Chem.* **1997**, *75*, 996.

(9) Yates, B. F.; Bouma, W. J.; Radom, L. *J. Am. Chem. Soc.* **1987**, *109*, 2250 and references therein.

(10) Brooks, B. R.; Schaefer, H. F. *J. Chem. Phys.* **1977**, *67*, 5146.

(11) Sanders, W.A.; Lin, M. C. *Chemical Kinetics of Small Organic Radicals*; Alfassi, Z., Ed.; CRC Press: Boca Raton, FL, 1988; Vol. III.

(12) James, F. C.; Choi, H. K. J.; Ruzsicka, B.; Strausz, O. P.; Bell, T. N. *Frontiers of Free Radical Chemistry*; Pryor, W. A., Ed.; Academic Press: Nwe York, 1980.

(13) Frisch, M. J.; Trucks, G. W.; Schlegel, H. B.; Gill, P. M. W.; Johnson, B. G.; Robb, M. A.; Cheeseman, J. R.; Keith, T.; Petersson, G. A.; Montgomery, J. A.; Raghavachari, K.; Al-Laham, M. A.; Zakrzewski, V. G.; Ortiz, J. V.; Foresman, J. B.; Cioslowski, J.; Stefanov, B. B.; Nanayakkara, A.; Challacombe, M.; Peng, C. Y.; Ayala, P.Y.; Chen, W.; Wong, M. W.; Andres, J. L. ; Replogle, E. S.; Gomperts, R.; Martin, R. L.; Fox, D. J.; Binkley, J. S.; Defrees, D. J.; Baker, J.; Stewart, J. P.; Head-Gordon,; M. Gonzalez, C.; Pople, J. A. *Gaussian 94W*; Gaussian, Inc.: Pittsburgh PA, 1995.

(14) (a) Moller, C.; Plesset, M. S. *Phys. Rev.* **1934**, *46*, 618. (b) Pople, J. A.; Binkley, J. S.; Seeger, R. *Int. J. Quantum Chem., Symp.* **1976**, *10*, 1.

(15) Hehre, W. J.; Radom, L.; Schleyer, P.v. R.; Pople, J. A. *Ab initio Molecular Orbital Theory*; Wiley: New York, 1986.

(16) Wang, Z.-X.; Huang, M.-B. Submitted.

(17) Wang, Z.-X.; Huang, M.-B. To be submitted.